

REPORT DOCUMENTATION PAGE

Form Approved
OMB No. 0704-0188

Public reporting burden for this collection of information is estimated to average 1 hour per response, including the time for reviewing instructions, searching existing data sources, gathering and maintaining the data needed, and completing and reviewing the collection of information. Send comments regarding this burden estimate or any other aspect of this collection of information, including suggestions for reducing this burden, to Washington Headquarters Services, Directorate for Information Operations and Reports, 1215 Jefferson Davis Highway, Suite 1204, Arlington, VA 22202-4302, and to the Office of Management and Budget, Paperwork Reduction Project (0704-0188), Washington, DC 20503.

1. AGENCY USE ONLY (Leave Blank)		2. REPORT DATE July 28, 1998	3. REPORT TYPE AND DATES COVERED Final January 1 through June 30, 1998	
4. TITLE AND SUBTITLE Communication Channel Propagation Model Based on a Combination of GTD and SBR			5. FUNDING NUMBERS DAAG55-98-C-0020	
6. AUTHORS Joseph Schuster and Raymond Luebbers				
7. PERFORMING ORGANIZATION NAME(S) AND ADDRESS(ES) Remcom Inc. Calder Square Box 10023 State College, PA 16805			8. PERFORMING ORGANIZATION REPORT NUMBER Remcom R98-101-006	
9. SPONSORING / MONITORING AGENCY NAME(S) AND ADDRESS(ES) US Army Research Office Attn: AMXRO-ICA (Sylvia Hall) 4300 S. Miami Blvd, P.O. Box 12211 Research Triangle Park, NC 27709			10. SPONSORING / MONITORING AGENCY REPORT NUMBER AR037898.1-EL-S&I	
11. SUPPLEMENTARY NOTES The views, opinions and/or findings contained in this report are those of the author(s) and should not be construed as an official Department of the Army position, policy or decision, unless so designated by other documentation.				
12a. DISTRIBUTION / AVAILABILITY STATEMENT Approved for Public Release; Distribution Unlimited			12b. DISTRIBUTION CODE	
13. ABSTRACT (Maximum 200 words) Report Developed under SBIR Contract. During Phase I significant extensions and improvements to our SBR/GTD propagation model have been made. An extended two-dimensional (2D) model has been developed that can be used in many situations to provide accurate results with less computer time than the fully 3D model. These include situations such as where the transmitting/receiving antennas are low, but there is propagation over buildings or hilly terrain. The computation time for all models (2D, extended 2D, and 3D) has been considerably reduced using several acceleration techniques. These include a faster path construction algorithm and improvements in the procedure for reusing diffracted path data. Considerable effort has been expended in providing fast and accurate predictions for rough terrain environments. Thus the SBR/GTD model can be used in situations where both building reflection/diffraction and terrain interactions with the electromagnetic fields are important. Another significant accomplishment was the validation of the SBR/GTD model by comparison with full wave results calculated using the Finite Difference Time Domain (FDTD) method. In addition to validation, the FDTD results can be used to improve the accuracy of the GTD diffraction coefficients and therefore of the SBR/GTD propagation predictions. Validation of the SBR/GTD model was also performed for several new cities, with excellent agreement between the SBR/GTD model results and measurements reported in the literature. Our Phase II proposal was written and submitted.				
14. SUBJECT TERMS SBIR Report Propagation			15. NUMBER OF PAGES 22	
			16. PRICE CODE	
17. SECURITY CLASSIFICATION OF REPORT UNC	18. SECURITY CLASSIFICATION OF THIS PAGE UNC	19. SECURITY CLASSIFICATION OF ABSTRACT UNC	20. LIMITATION OF ABSTRACT	

Final Technical Report

July 1998

Communication Channel Propagation Model Based on a Combination of GTD and SBR

SBIR Contract Number: DAAG55-98-C-0020

Report Number R98-101-006

Submitted to
Department of the Army
U. S. Army Research Office
P. O. Box 12211
Research Triangle Park, NC 27709-2211

Submitted by
Joseph W. Schuster and Raymond J. Luebbers
Remcom, Inc.
Calder Square, Box 10023
State College, PA 16805

Phone: 814-353-2986
Fax: 814-353-1420
E-Mail: jws@remcom.com

19990104 085

1. Background and Introduction

Modeling the constantly changing communication channel between on-the-move vehicles is a more computationally challenging problem than modeling propagation within commercial cellular and PCS systems. The added difficulty arises mainly out of the fact that both ends of the communication link are now mobile. In most commercial applications predictions might be made for many field points, but the source points are at a rather small number of fixed base station positions. But for mobile-to-mobile predictions, there will be a need to consider as many source points as field points since either vehicle can in general be anywhere within the area. The propagation prediction approach developed by Remcom, Inc. is a combination of the Shooting and Bouncing Ray (SBR) method and the Geometrical Theory of Diffraction (GTD). This approach is well suited to making mobile-to-mobile propagation predictions and is also efficient for commercial cellular/PCS systems with fixed base stations.

The SBR method is first employed as the basis of a ray-tracing procedure to determine the geometrical ray paths through the building and terrain geometry. Because the SBR paths are traced without regard for the location of specific transmitters (Tx) or receivers (Rx) locations, this approach to ray tracing is well suited to applications in which there may be a need to evaluate the communication link for thousands of Tx/Rx pairs. Both the 2D and 3D implementations of this approach are robust ray-tracing techniques that impose no limitations on the complexity of the building or terrain geometries. During Phase I several improvements have been made in the acceleration techniques that are used to reduce the computer time for the SBR portion of the computations.

A number of researchers have developed two-dimensional models to take advantage of the fact that in a typical urban area the transmitting and receiving antennas may frequently be well below most of the building heights. By ignoring propagation paths over the buildings it is possible to restrict the ray tracing to a single horizontal plane using the building "footprints" to determine the ray paths. The weakness of this approach is that even when only a few buildings violate the tall building approximation, the model can lead to inaccurate results. During Phase I, we have developed a partial 3D model which is able to predict propagation paths over low buildings, but which still uses 2D ray tracing. Propagation over uneven terrain can also be predicted with a variation of this model. We are still investigating the limitations of this approach to determine applicability for different types of terrain.

During Phase I we have employed the finite difference time domain (FDTD) method as a tool for evaluating the accuracy of our SBR/GTD codes. A preliminary two-dimensional FDTD analysis made during Phase I has revealed larger than expected errors in the widely used finite conductivity Uniform Theory of Diffraction (UTD) wedge diffraction coefficients [1]. While these coefficients are still considerably more accurate than the knife-edge diffraction formulation or the perfect conductor UTD coefficients, the FDTD comparisons have shown that substantial errors can still occur when the diffracted ray is not near the shadow boundaries. This result has indicated an area of potential improvement in model accuracy which we intend to exploit in Phase II. We have also begun to use FDTD as a tool for evaluating the accuracy of the ray-tracing algorithms and for gaining insight into diffuse scattering from rough surfaces.

2. Quasi 3D Model based on 2D Ray Tracing

During Phase I, a quasi three-dimensional model has been developed which can predict propagation paths over low buildings and hills, but still employs fast 2D ray-tracing using the footprints of the buildings. Prior to this work, the 2D model could only be used when the terrain was flat and the transmitting and receiving antennas were well below all the building heights. When these conditions were not satisfied, accurate predictions required using a slower fully three-dimensional model. Our new quasi 3D model is much faster because the ray-tracing is still confined to a single horizontal plane even though rays can propagate vertically. The rays which propagate over roof-tops appear to go through the buildings in the horizontal plane, but the model then evaluates them including the vertical plane propagation effects. This quasi 3D model is not intended to replace the full 3D model, which is still required when antennas are much higher than many of the buildings, or for areas with an extremely hilly or mountainous terrain.

The quasi 3D model can predict line-of-sight (LOS), singly diffracted, and doubly diffracted paths over buildings. These paths can also include reflections from the building walls and diffractions from the vertical edges, with these interactions occurring before or after the path passes over a building roof. The model is most accurate when the paths are near the horizontal plane, but the paths are not assumed to lie on any particular plane as they are in the "slant plane" approaches tried by other researchers. A simple example of propagation over a building rooftop by means of a single diffraction is shown in Figure 1. The path clears the left-hand side of the building but must reach the receiver by diffracting at the right-hand wall down to street level. A weaker path which diffracts at both edges of the roof would also exist. But if the transmitter was lowered sufficiently, the only path would be the doubly diffracted path. On the other hand, if the transmitter was raised sufficiently, a LOS path would exist. The quasi 3D model would be applicable to all of these situations.

The validity of using this approach for constructing these additional paths depends on several assumptions. The first is that the new paths do not lie far from the ones initially traced out by the transmitted rays, so the distance by which the paths are being displaced vertically is small compared to the total path length. This will be true when the vertical separation between the transmitter and receiver is small compared to the horizontal separation. The second assumption concerns the basic nature of an urban building geometry. In an urban area the buildings will often be very complex in the horizontal plane, but not nearly so complex vertically. The fact that almost all buildings have flat vertical walls guarantees that the strongest paths will lie close to the horizontal plane because there are no interactions which can scatter a significant amount of energy from a vertically-propagating ray back into this plane. This assumption makes it possible to construct the paths which have propagated over the lower buildings by considering the height at which the rays intersected the building faces. However, it is not necessary to assume that all the buildings are vertically uniform, and structures such as the tall tower in the center of the building on the right in Figure 1 would still block propagation paths.

The propagation paths over the rooftops are found by first tracing both transmitted and reflected rays through all buildings. Although the LOS path may be the strongest, in many situations all possible paths need to be considered. For example, Figure 2 shows a situation in

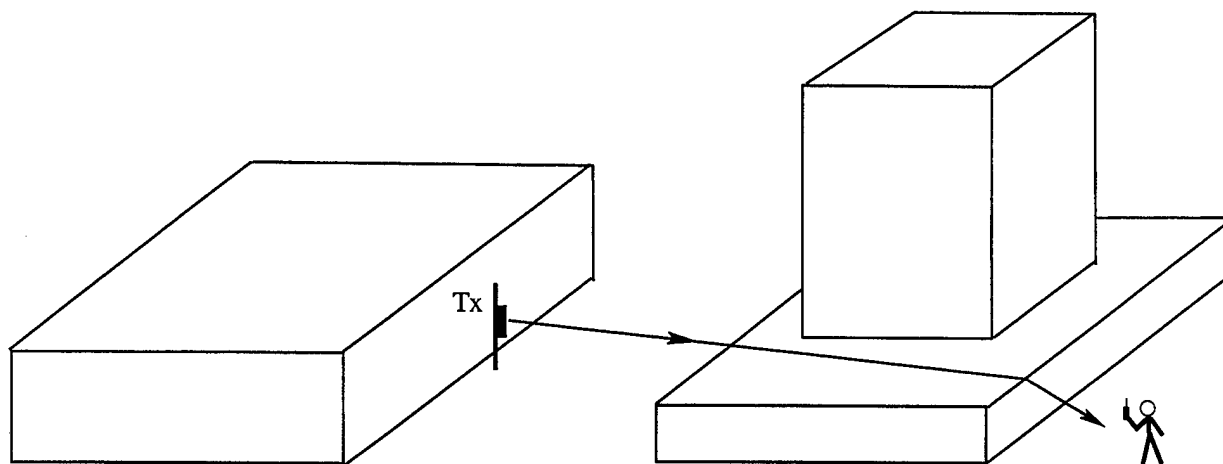


Figure 1: Propagation over a building rooftop by a single diffraction

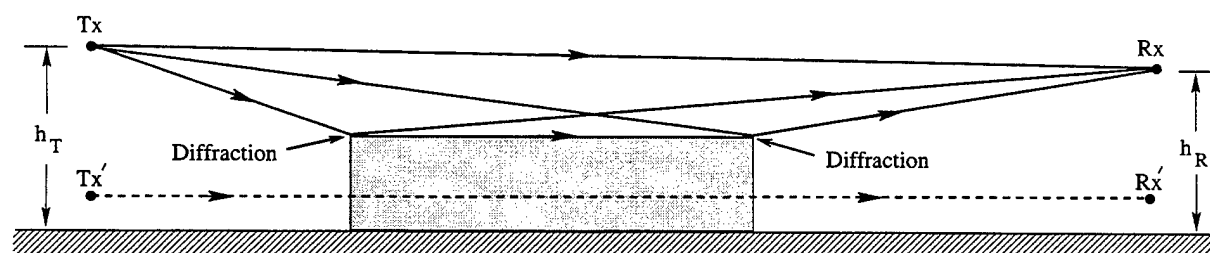


Figure 2: The four ray paths by which energy can propagate over a building when the transmitter and receiver are above the roof of the building.

which a LOS path, two singly diffracted paths, and a doubly diffracted path would be constructed. For clarity, the transmitter and receiver heights relative to the building height have been exaggerated, but in a typical situation the antennas would not be so much higher than the building. All four paths in Figure 2 are present only when both antennas are above the building. When either the receiver or transmitter are below the roof of the building, one of the singly diffracted paths, and possibly the LOS path, will be blocked, and if both antennas are below the building the only path considered is the doubly diffracted one. Because the path data is always stored in memory or on the hard disk, the signal strength can be recalculated very quickly for these different antenna heights, since it is not necessary to perform any additional ray tracing.

An accurate evaluation of the signal strength requires that all paths be combined coherently, in order to take into account the way the paths interfere according to the GTD. The single diffractions can be evaluated using the finite conductivity wedge diffraction coefficients in [1], but the double diffractions require the finite conductivity slope diffraction coefficients in [2].

The over-rooftop rays will usually be oblique to the diffracting edge, and comparison to the full 3D model have shown the quasi 3D model is generally able to predict this angle accurately. This angle is required to correctly evaluate the diffracted fields with UTD.

Comparison with the full 3D code have been used to validate this approach using the measurements made in Rosslyn, Virginia, for Tx site 8 in Figure 3. Figure 4 compares the full 3D model and the quasi 3D model to the measured path loss at 900 MHz. The free space path loss has also been included to illustrate the large additional attenuation that occurs due to the buildings.

3. Acceleration of the Ray-Tracing Process

Our Phase I effort has concentrated on extending our existing prototype propagation models to provide fast predictions for mobile-to-mobile radio communications in complex environments. In the typical application in which predictions are to be made for a large number of Tx/Rx points in an urban geometry, the rays are initially traced from all the building edges with the rays reflecting specularly from the building faces. For a mobile-to-mobile calculation, no distinction is made between Tx and Rx points during the ray tracing process. After the SBR paths from each edge are found, the next step is to construct the propagation paths from the edge to the Tx/Rx points and to other edges. These partial paths form a database from which the complete diffracted paths can be later determined between any two points without additional ray-tracing.

In the approach we have developed, the construction of the singly diffracted paths involves three steps. The first step is the actual ray-tracing using the SBR technique, the second is the construction of the propagation paths from the diffracting edges to the Tx/Rx points, and the third is the construction of the complete Tx to Rx path. This division allows for a large reduction in the computation time through the reuse the geometrical path data obtained with the ray-tracing. The data from the second step is stored on the hard disk and reused repeatedly for determining the paths for different Tx/Rx pairs. This approach makes use of the fact that the path to the Rx following the diffraction does not change as the source point moves, so it is only

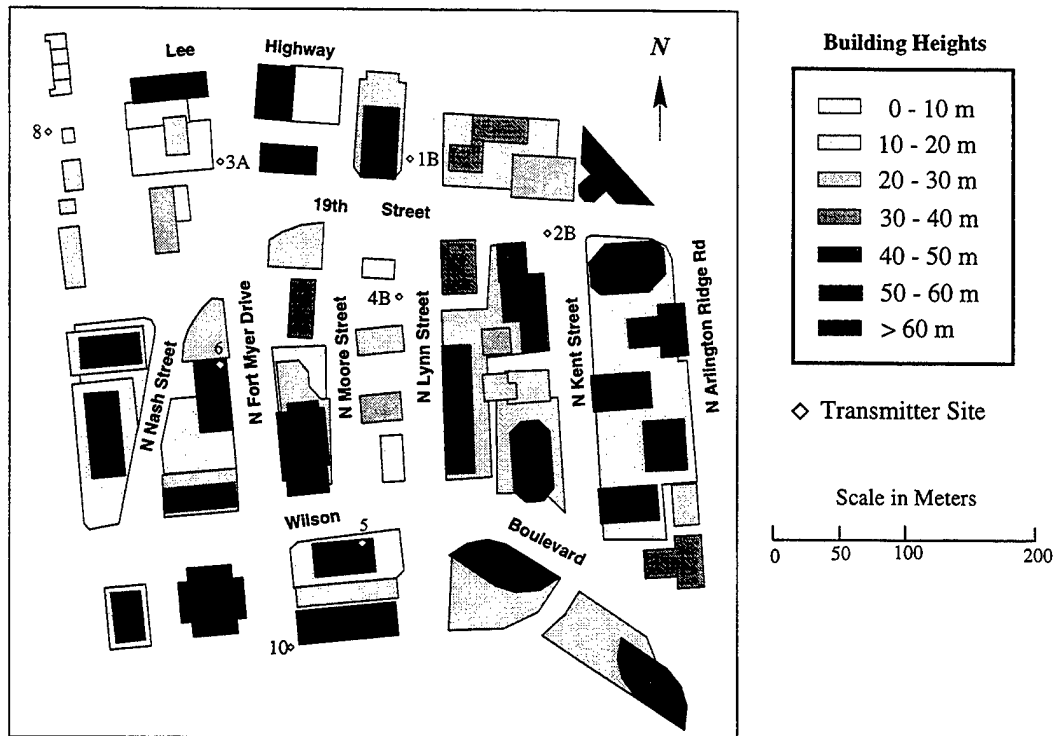


Figure 3: Plan view of the high rise area of Rosslyn, Virginia showing building locations, building heights relative to the local ground and transmitter sites.

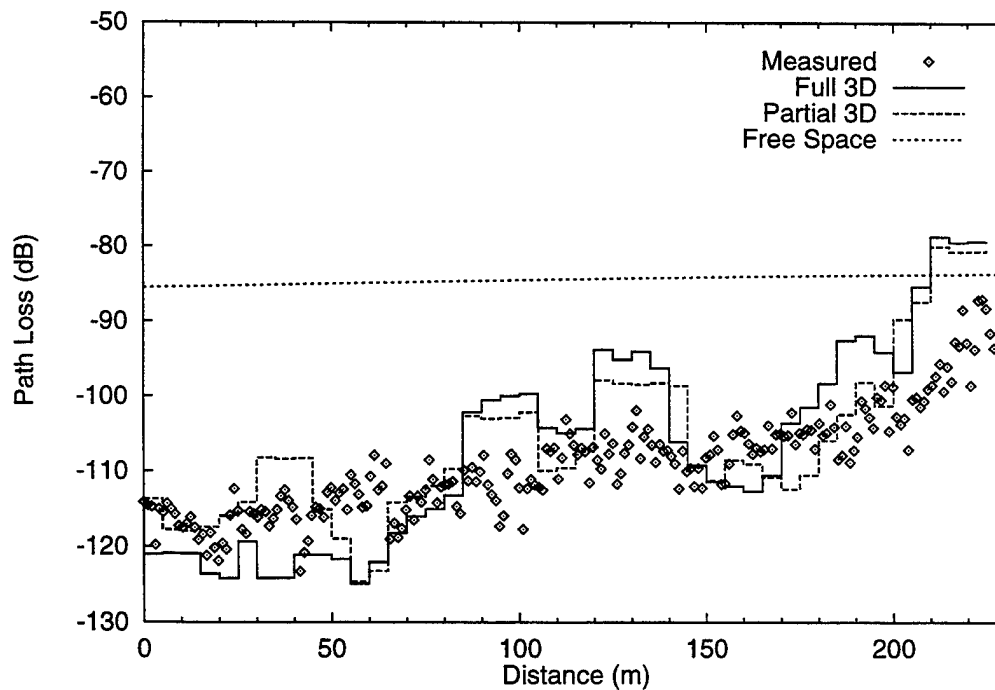


Figure 4: Path loss at 900 MHz along Kent St. with the transmitter at site 8.

necessary to combine the paths before and after the diffractions, which can be done very quickly. The geometrical paths do not depend on the antenna patterns, polarizations, frequency, or building dielectric parameters.

To provide for flexibility, the propagation prediction computer codes have been written using a modular programming style. It is also possible to add Tx and Rx points to the data base after the initial ray-tracing procedure has been executed.

On computers with at least 128 MB of RAM it may be possible to keep all the paths in RAM. However this will not always be the case, and it is crucial to access this data quickly from the hard drive. The paths can be written to the hard disk to be read back into the propagation program at a later time for additional analysis. This does not require a large amount of disk space by today's standards. For example, the storage requirements for 2000 or so field points along the streets of a one square mile urban area would be 20-50 MB.

The shooting and bouncing approach to ray tracing can be slow if it is necessary to check a large number of faces to find the reflection points of each ray. The solution to this is not simply using a larger angular spacing between rays. This can lead to serious errors such as entirely missing interactions with buildings or incorrectly predicting the multipath contributions at distant field points. With our approach fast results are obtained by accelerating the ray tracing using techniques which do not compromise the accuracy. These acceleration techniques make use of several parameters which relate the building positions and orientations to one another. The ray tracing algorithm uses this information to predict the most likely reflections points and then these are checked first. This greatly reduces the number of building or terrain faces which have to be checked.

Once the SBR paths have been found, the next step is to construct the specific ray paths to each field point. This is done by enclosing each field point by a collection surface and finding the SBR rays which intersect these surfaces. Since a number of SBR rays which have followed essentially the same path through the buildings or terrain may intersect this collection surface, the rays are sorted to select just one ray for each unique path. The run time for the collection process has been reduced by grouping the Tx/Rx points within larger bounding boxes and first considering the intersections of groups of rays with these bounding boxes. Only if an intersection is found are individual rays and field points within the bounding boxes checked.

4. Rough Terrain Propagation Model

In several papers from the 1980s [1, 3-5] the superior accuracy of finite conductivity UTD diffraction coefficients for propagation over rough terrain was demonstrated relative to knife-edge diffraction formulations and semi-empirical methods. These predictions were made using a 2D piecewise linear approximation to the terrain and the ray paths were determined using a multiple image approach.

During Phase I, the application of a two-dimensional SBR approach to ray-tracing for rough terrain was investigated and a prototype code was written. The SBR based ray-tracing technique has been modified slightly to make it more efficient in rough terrain environments. To avoid shooting an unnecessarily large number of rays, it is more efficient to launch a much higher

density of rays near the horizontal plane, since it is mainly these rays which will provide the ray paths to distant diffracting edges or field points. If too large of a spacing between rays is used entire terrain faces may be missed during the ray tracing.

This 2D rough terrain model has initially been developed for situations in which the terrain can be approximated by a two-dimensional profile, and the Tx and Rx points lie on a single vertical plane perpendicular to the ridges. The approach was later extended to situations in which the Tx and Rx points lie on a plane oblique to the parallel ridges. For accurate predictions in these situations, it is necessary to include the oblique incidence angle when evaluating the UTD diffraction coefficients. In order to avoid using the slower full 3D model to predict these paths, we have developed an algorithm to estimate these angles using a 2D ray-tracing and the terrain geometry. The limits of this approach have been evaluated by means of comparisons to the full 3D model.

This vertical plane model has been compared to path loss measurements in several papers [1,3-5] written by Raymond Luebbers. The predictions in these papers were made using the same finite conductivity UTD wedge diffraction coefficients currently used in Remcom's SBR/GTD model. The only difference is that the ray paths are now found using the SBR technique rather than the multiple image method. The new predictions, as expected, are in very good agreement with the earlier predictions, and both are in good agreement with the measurements.

The SBR/GTD approach has also been extended to predict propagation paths with three diffractions. These paths are constructed from simpler path segments in the same way in which the single and double diffracted paths are found. No additional ray-tracing is required to find the triply diffracted paths. Paths with more than three diffractions could also be constructed with this approach, but we do not plan to implement this capability until a need for it is demonstrated. The electric field amplitude of the triple diffractions is evaluated using the UTD formulation in [3].

In order to apply GTD it is first necessary to construct piecewise-linear terrain profile. A prototype computer code has been developed during Phase I for automating the construction of a linearized terrain profile starting from digitized terrain data on a rectangular grid. An iterative approach is used to find the least squares fit to the terrain data. The linearized profile which is constructed only incorporates large scale terrain features which can significantly effect the propagation paths.

5. Full 3D Propagation Model

During Phase I significant improvement in the calculation speed of the model was achieved, especially for the 3D version. This has been accomplished mainly through the implementation of ray-tracing acceleration technique borrowed from 3D computer graphics. These techniques had previously been implemented in the 2D ray-tracing. This work will continue during the last two months of Phase I. During Phase II we intend to further reduce the model calculation time. This will require some restructuring of the computer code. In conjunction with this restructuring, the code will be modified so that calculation arrays can be

dynamically allocated. This will allow delivery of the code as an executable module. Several ray tracing acceleration techniques were previously developed and implemented for the 2D ray tracing used in the quasi 3D model and 2D rough terrain model. These techniques are used to greatly reduce the number of ray-polygon intersection tests which need to be performed to find the reflection points of each ray. These techniques have now been implemented in the full 3D code. The techniques that are used include: bounding boxes, spatial partitioning, depth-sorting of faces, and angular z-buffering.

When a shooting and bouncing ray (SBR) method is used as a ray tracing procedure, one cannot initially evaluate the field at a particular point, since no SBR rays will ordinarily pass exactly through that point. Instead, a collection surface enclosing the field point is defined, and then the rays that pass through this surface are used to construct the specific GO and GTD ray paths to the field point. In the most straightforward implementation, all rays would have to be checked for an intersection against all the collections surfaces. As with the ray tracing, the computation time is reduced by limiting the number of times the full intersection computations are performed. This is accomplished by grouping field points within larger bounding boxes and first considering the intersections of groups of rays with these bounding boxes. Only if an intersection is found are individual rays and field points checked.

The implementation of these acceleration techniques has significantly reduced the computational time of the 3D model. For example, the run time for an approximately 500 m x 500 m urban area with 50 buildings and 500 Tx/Rx points along the streets is now 20 minutes on a computer with a 200 MHz Pentium Pro processor. This calculation found propagation paths with up to six reflections and one diffraction. The same calculation would have previously required over two hours. Improvements in how the various acceleration techniques are used in conjunction with each other are expected to result in further reductions.

6. Validation

Our basic approach to urban radio propagation prediction was previously validated by comparisons with measurements made over a two year period in Rosslyn, Virginia, a suburb of Washington DC [6,7]. Rosslyn is a complex urban area which contains a variety of building shapes and sizes. Our propagation model was initially applied to the primarily high-rise environment, and then later applied to mixed commercial and residential areas. These measurements were all made for fixed base stations with predictions of the path loss compared to measurements at thousands of points along the streets. The measurements were made by a group at AT&T Bell Laboratories. All predictions were made blind, that is, the predictions were submitted to the group at AT&T and to the sponsor before the measured data was received.

The high rise area of Rosslyn in which many of these measurements were made is shown in Figure 3. Comparisons of path loss measurements to blind predictions made with the 2D and 3D versions of the SBR/GTD model are shown in Figures 4-7. These results are representative of the agreement that was obtained. The free space path loss is included in these plots to show the large additional attenuation introduced by the buildings.

This work will be discussed briefly in the section below on related work. The highly accurate

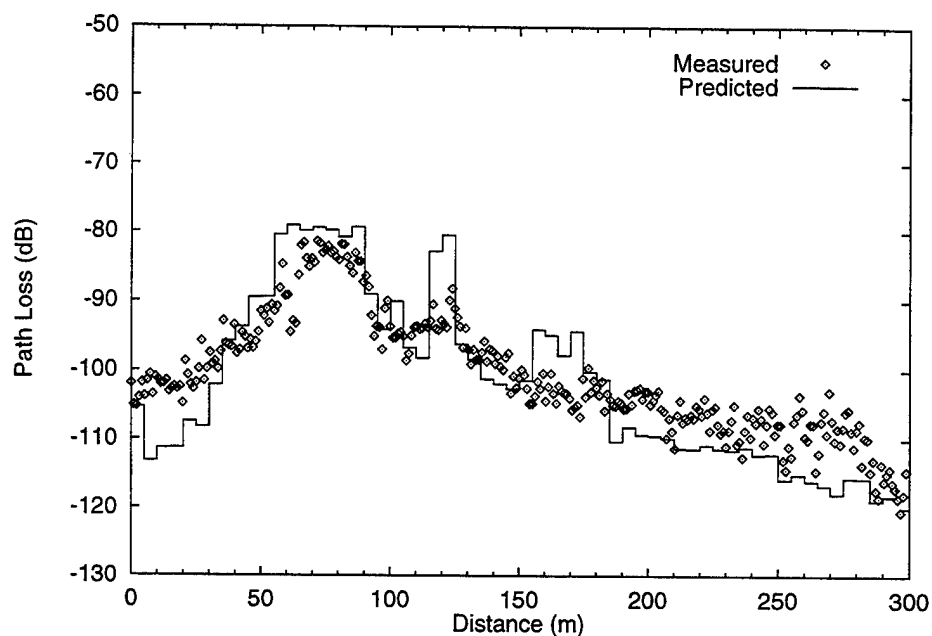


Figure 5: Path loss predictions by the 3D SBR/GTD model along Lynn St. at a frequency of 1.9 GHz with the transmitter on a rooftop at site 6. The path starts at Wilson Blvd. and ends at the Lee Hwy.

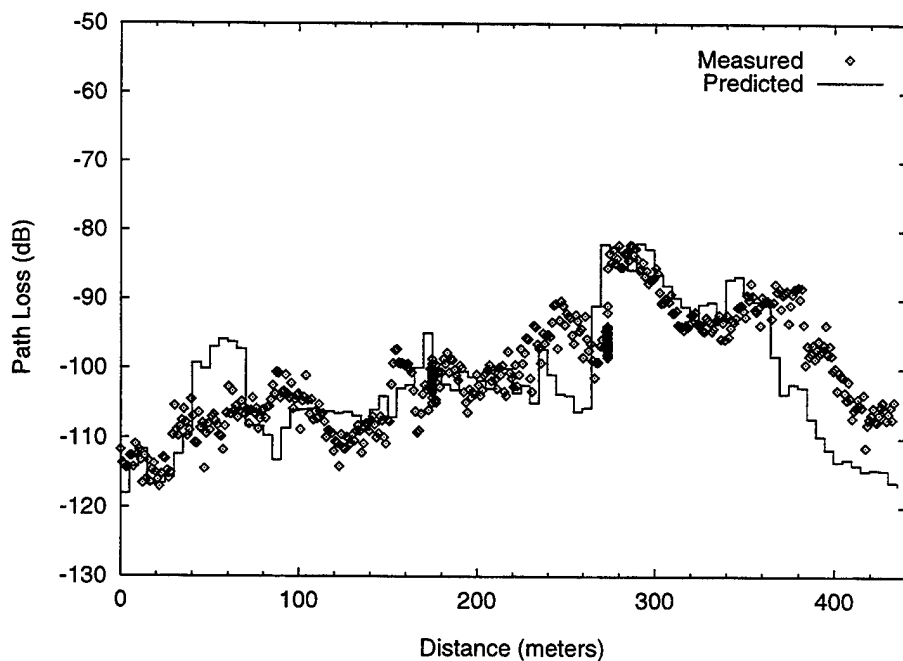


Figure 6: Path loss predictions by the 3D SBR/GTD model along Nash St./19th St. at a frequency of 1.9 GHz with the transmitter on a rooftop at site 5. The path starts at Wilson Blvd. and ends at Kent St.

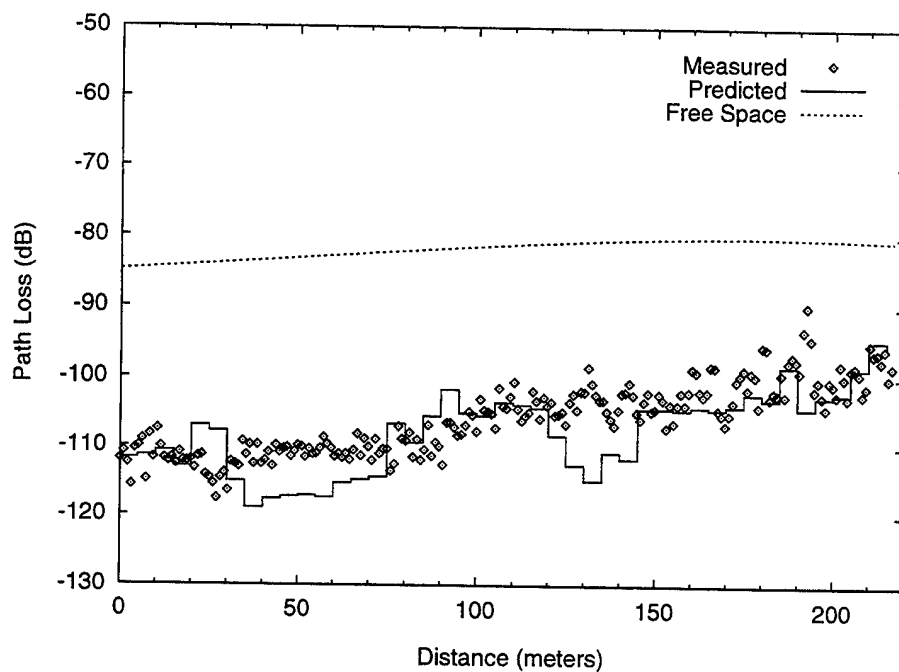


Figure 7: Path loss predictions by the 2D SBR/GTD model along Kent St. at a frequency of 900 MHz with an omnidirectional transmitting antenna at site 4B, 10 m above local ground. The path starts at Wilson Blvd. and ends at 19th St.

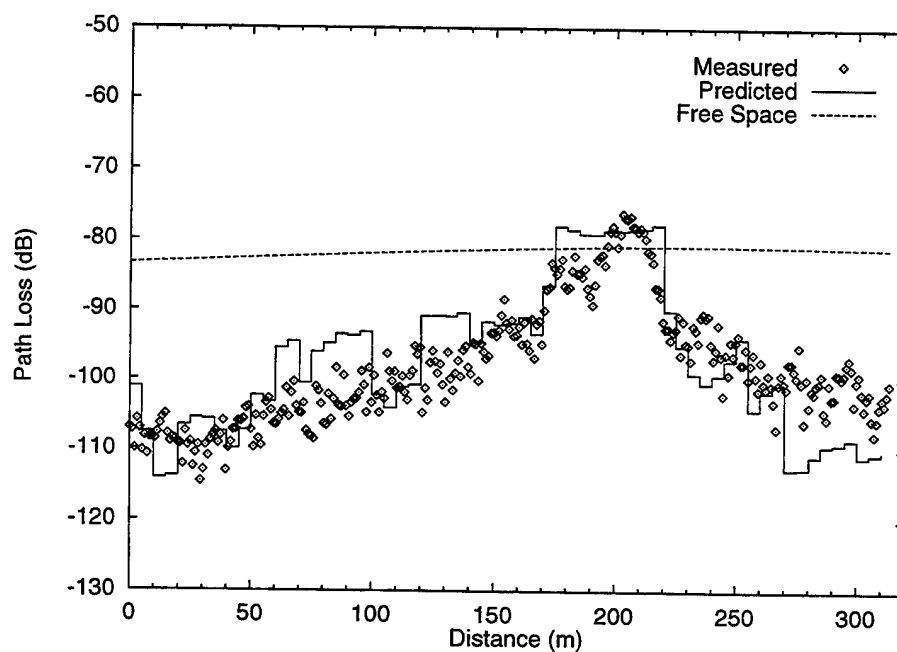


Figure 8: Path loss predictions by the 3D SBR/GTD model along Lynn St. at a frequency of 900 MHz with an omnidirectional transmitting antenna at site 8, 10 m above local ground. The path starts at Wilson Blvd. and ends at the Lee Hwy.

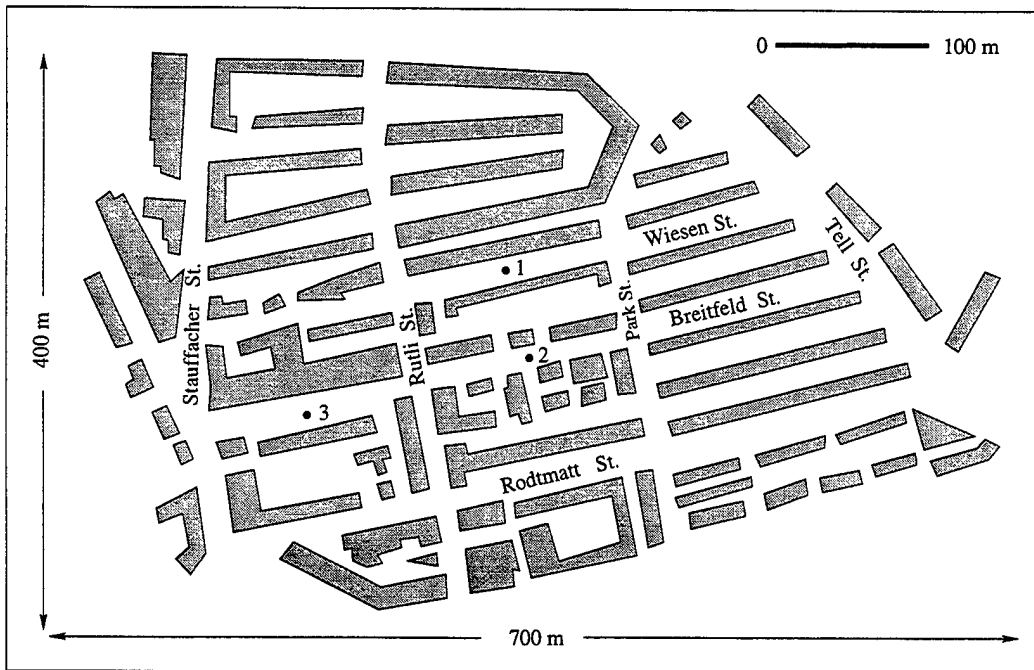


Figure 9: Bern, Switzerland

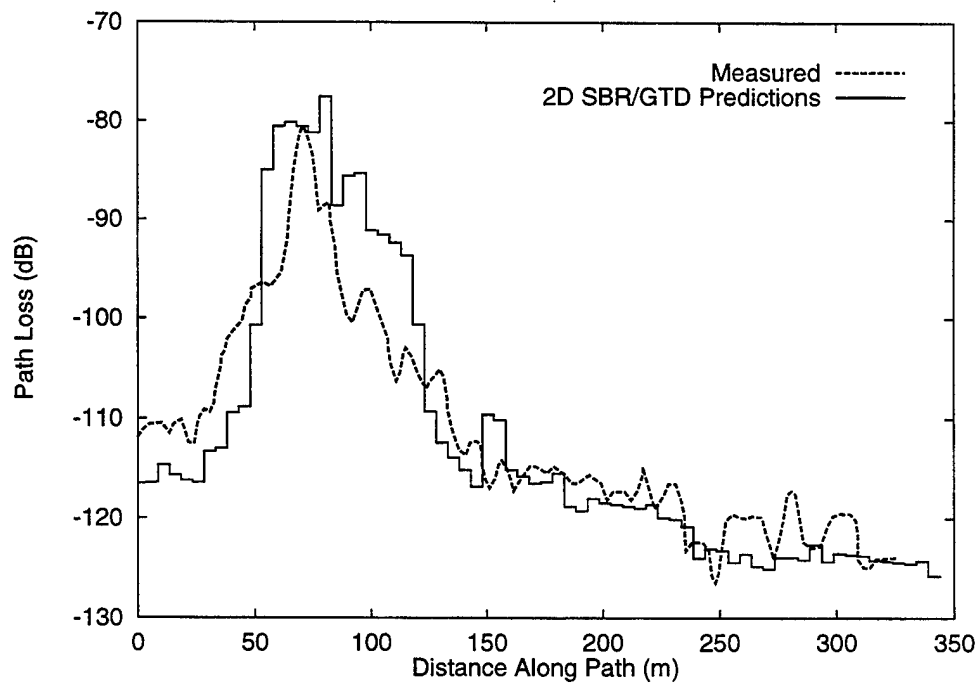


Figure 10: Comparison to measured path loss along Stauffacher St. at 1.9 GHz with the transmitter at site 2

building and terrain data which was obtained for the Rosslyn area has been used in the Phase I research to provide a realistic environment against which to validate improvements in our propagation model.

We have also attempted to make comparisons to published measurements in the technical literature. However, these measurements are often presented in a manner that makes comparison difficult. An exception is a recent paper in which comparisons to measurements were made within residential sections of Bern and Fribourg, Switzerland [8]. This paper contains excellent maps of the two areas, legible plots of measurements and the authors' predictions, and a complete description of the measurement equipment and procedure. The building geometry for Bern is shown in Figure 9. Our 2D SBR/GTD code was found to be in good agreement with these measurements. Some sample results are shown in Figure 10.

7. Using FDTD to Validate and Improve Accuracy

A number of 2D ray-tracing based models for making site-specific propagation predictions in urban microcells have been described in recent publications. These models have usually been compared to path loss and delay spread measurements. However, because of the complexity of the environments in which the measurements are made, it is often not clear from the comparisons why the predictions are inaccurate in some areas and how the models can be improved. The fact that the measurements are subject to large uncertainties which are difficult to quantify also makes it difficult to draw definite conclusions about the accuracy of the models from measurements.

One goal of our Phase I work with FDTD has been to develop techniques by which it can be used to evaluate the accuracy of ray-tracing based propagation models. Some of these results have been presented in [9]. The FDTD method is a direct implementation of Maxwell's Equations without the high frequency approximations used in the GTD. Thus FDTD is taken as the true accurate solution and is used to validate the GTD results.

Although the building geometry can be approximated as two-dimensional, the fields will still attenuate with distance from a point source as spherical waves. However, the 2D FDTD simulation actually models a line source, and the calculated fields will spread with distance as cylindrical waves. Therefore, to compare the FDTD fields directly to measurements or to the GTD predictions it is necessary to modify the FDTD fields to have the correct spherical wave attenuation with distance. We have developed an approach for converting the 2D FDTD results to predict 3D propagation.

For non-diffracted fields which reflect only from planar surfaces, the spreading is as $1/r$ for spherical waves and as $1/\sqrt{r}$ for cylindrical waves, where r is the total path length. For diffracted fields the attenuation with distance is more complicated, but from the geometrical theory of diffraction it can be shown that the ratio of the spherical to cylindrical wave attenuation remains $1/\sqrt{r}$. Our approach is based on the fact that in free space $r = ct$, and we introduce an additional attenuation factor of $1/\sqrt{r}$ into the FDTD fields by multiplying the time domain fields by $1/\sqrt{ct}$. This has been implemented by exciting the FDTD simulation with a narrow pulse at the source point and then saving the complete time record at each point of

interest. In post-processing the fields are multiplied by the correction factor and then Fourier transformed to obtain the amplitudes and phases of the frequency domain fields.

To demonstrate what can be learned from these comparisons, consider the simple geometry in Figure 11 consisting of four buildings with a rectilinear street pattern. Each building consists of a perfect electrical conducting core with a 0.3 m thick lossy dielectric coating ($\epsilon_r = 4$, $\sigma = 0.05$ S/m) on all sides. A cell size of 1.5 cm (20 cells per wavelength at 1 GHz) was used in the FDTD simulation.

A vertically polarized field was excited at $x=37.5$, $y=6.2$ m. To prevent the excitation of unwanted low frequency fields which GTD cannot predict, the FDTD simulations were excited with a truncated derivative of a Gaussian having the form

$$E(t) = \begin{cases} -2A_0\alpha(t - \beta\Delta t)e^{\alpha(t - \beta\Delta t)^2} & 0 \leq t \leq 2\beta\Delta t \\ 0 & t > 2\beta\Delta t \end{cases} \quad (1)$$

where $\alpha = [1/(\beta\Delta t/4)]^2$ and $\beta = 48$. In Figure 12 the FDTD and GTD calculated electric fields are compared at 900 MHz along the line CD in Figure 11. These results demonstrate the accuracy of the finite conductivity UTD diffraction coefficients.

An alternative is to compare the GTD and FDTD results in the time domain. This makes it possible to compare specific ray paths to the field point. Table 1 lists the building interactions and the time of arrival for the first ten significant GTD paths to arrive at receiver point number 1, and in Figure 13 the first five of these paths are plotted with the building geometry. Several paths (mainly double diffractions) which are of very low amplitude have been omitted from Figure 13 and the table. To give some indication of the strength of each path, the power in decibels relative to one milliwatt (dBm) for a transmitted power of 0 dBm are given at 500 MHz, which is approximately the center frequency of the excitation pulse.

The first ray to arrive at point 1 is one which diffracts twice, first from the lower left hand corner of building 2 and then from the upper right hand corner of building 1. There are several rays listed in Table 1 which travel nearly the same distance and arrive at nearly the same time as other rays. For instance, ray paths 2 and 3 differ only by path 3 having a second diffraction from building 1. Ray paths 5 and 6 are another such pair which follow nearly parallel paths.

It is interesting to note that ray 10 is the first ray to arrive at point 1 which undergoes only reflections and no diffractions, and due mainly to presence of the lossy building surfaces, this path is 10 dB weaker than path 5, which undergoes a diffraction but two less reflections. This demonstrates why diffraction rather than multiple reflection is often the most important propagation mechanism in the outdoor environment

To compare the GTD time domain response directly to the FDTD time domain results, the GTD time domain fields are determined from

$$E_{GTD}(t) = F^{-1}\{E_{GTD}(f) \times E_1(f)\}, \quad (2)$$

where F^{-1} denotes the inverse Fourier transform, $E_1(f)$ is the Fourier transform of the excitation

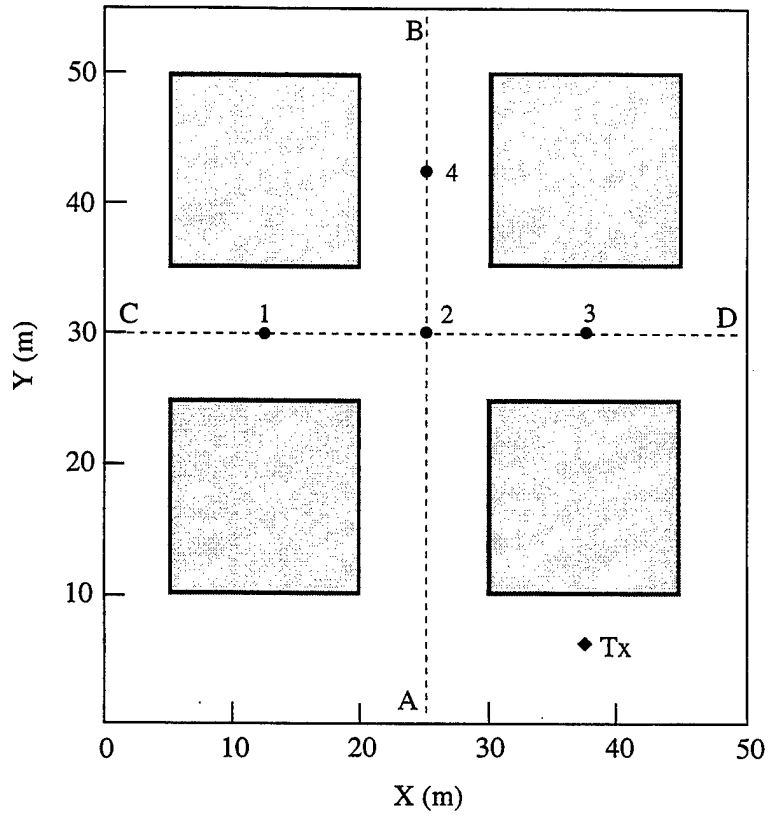


Figure 11: Four building geometry

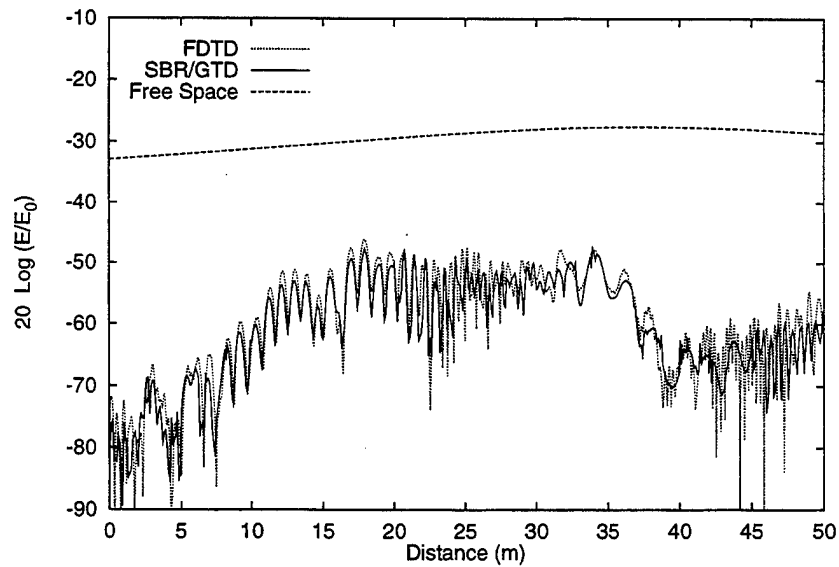


Figure 12: Comparison of the GTD and FDTD calculated electric fields at 900 MHz along the line C-D in Figure 3. The GTD fields include ray paths with up to 8 reflections and 2 diffractions.

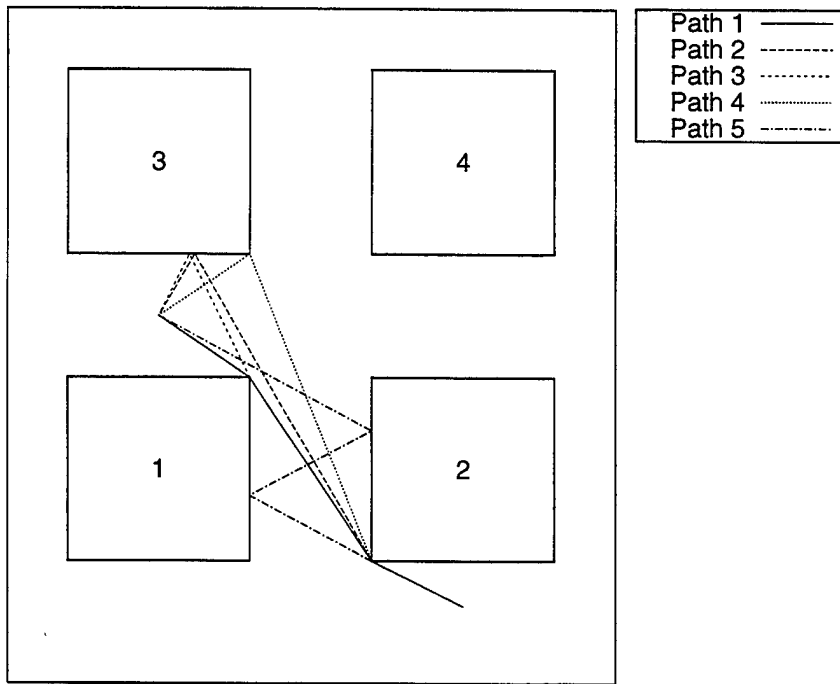


Figure 13: GTD ray paths to point 1

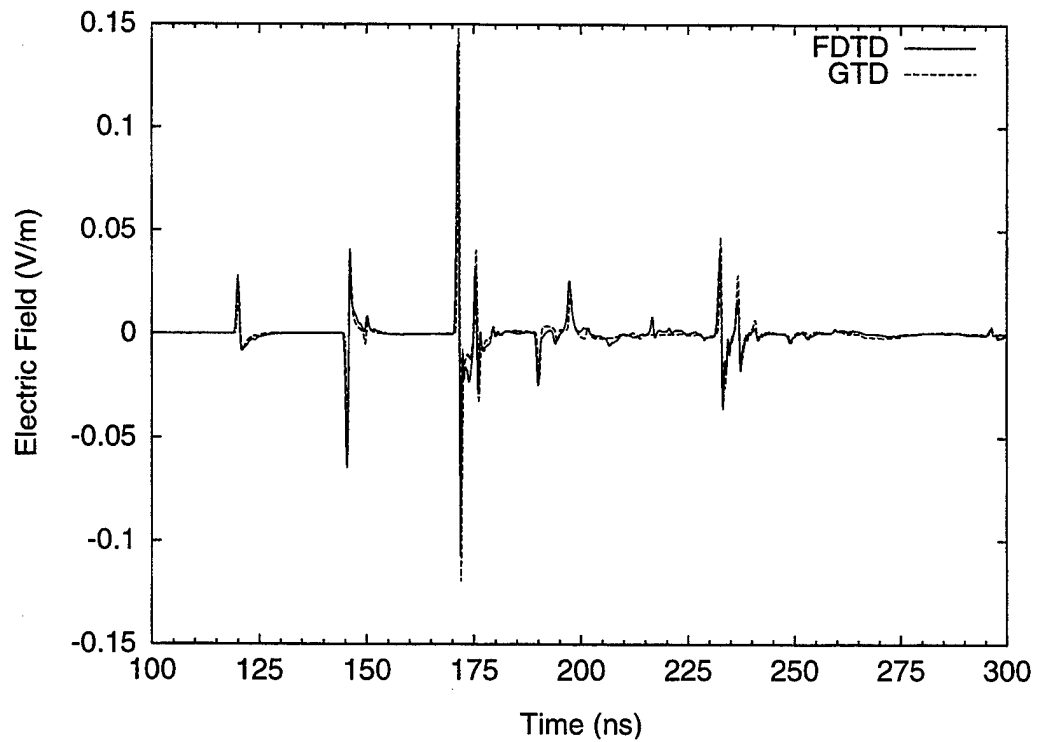


Figure 14: Comparison of FDTD and GTD time domain fields

pulse at one meter from the source point, and $E_{\text{GTD}}(f)$ is the frequency domain response evaluated using an electric field amplitude of 1 V/m at one meter from the source. The GTD time domain predictions are compared to the FDTD time domain fields in Figure 14. By referring to Table 1 and Figure 13, it is possible to associate specific ray paths with the peaks in the FDTD response. For example, the doubly diffracted ray which arrives first at point 1 at 118 ns is clearly present, and the amplitude and overall shape are in good agreement with the FDTD results.

Path	Sequence of Building Interactions	Time (ns)	Power (dBm)
1	Tx - D(2) - D(1) - Rx	118	-102.5
2	Tx - D(2) - R(3) - Rx	144	-91.8
3	Tx - D(2) - D(1) - R(3) - Rx	144	-101.2
4	Tx - D(2) - D(3) - Rx	148	-129.6
5	Tx - D(2) - R(1) - R(2) - Rx	170	-81.8
6	Tx - D(2) - R(1) - R(2) - D(1) - Rx	170	-90.9
7	Tx - D(2) - R(3) - R(2) - Rx	174	-103.5
8	Tx - D(2) - R(1) - D(2) - R(3) - Rx	188	-102.3
9	Tx - D(2) - R(1) - R(2) - D(1) - R(3) - Rx	196	-110.7
10	Tx - R(1) - R(2) - R(1) - R(2) - Rx	231	-91.6

Table 1: Arrival time and building interactions for the first 10 significant ray paths to point 1. In the second column, "D" denotes a diffraction, "R" denotes a reflection, and the numbers refer to the buildings in Figure 12.

To directly test the accuracy of the UTD finite conductivity diffraction coefficients consider the 90 degree wedge geometry in Figure 15. This consists of a PEC wedge coated with the same 0.3 m thick lossy dielectric material described above. This simple geometry was used to compare the finite conductivity UTD fields to the FDTD fields. The diffracted field is obtained by subtracting the geometrical optics fields from the total field. Figure 16 shows that the finite conductivity UTD and FDTD calculated fields are in very good agreement near the reflection shadow boundaries at 30 and 210 degrees, but in other directions there are large differences.

It may often be necessary to use simplified building shapes, either because of insufficiently accurate data or because of intentional simplification of the buildings in order to reduce the computation time. The effect these simplifications will have on the predictions has not been considered in the technical literature. Calculations with FDTD provides a means of determining how sensitive the propagation behavior is to building shape. To illustrate this, consider the following three corner shapes: (1) the "square" corner shown in Figure 15, (2) the

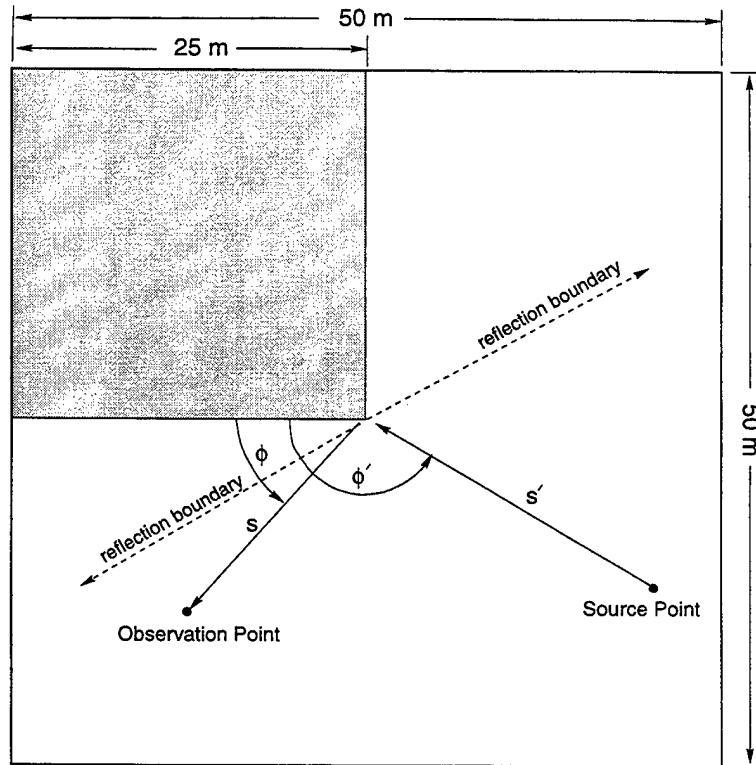


Figure 15: Geometry for comparing FDTD to finite conductivity UTD diffracted fields

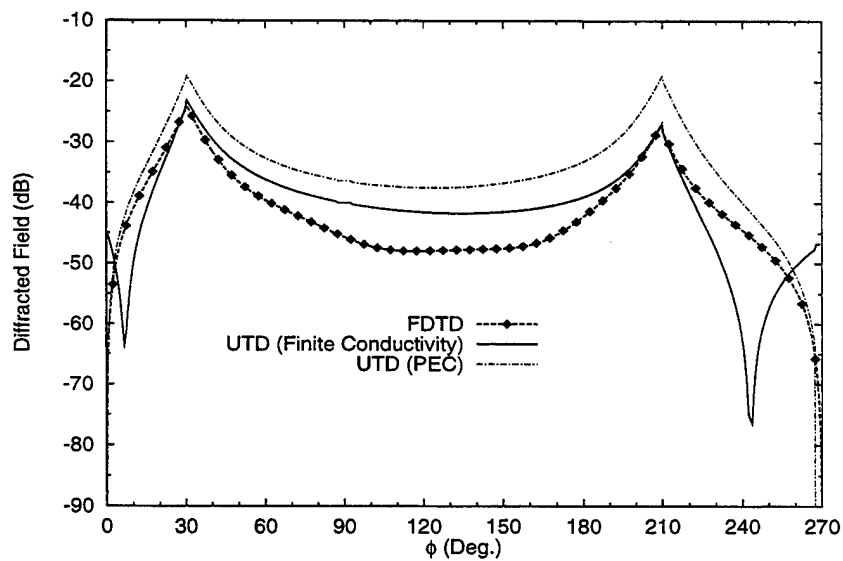


Figure 16: Comparison of finite conductivity UTD wedge diffracted fields to FDTD

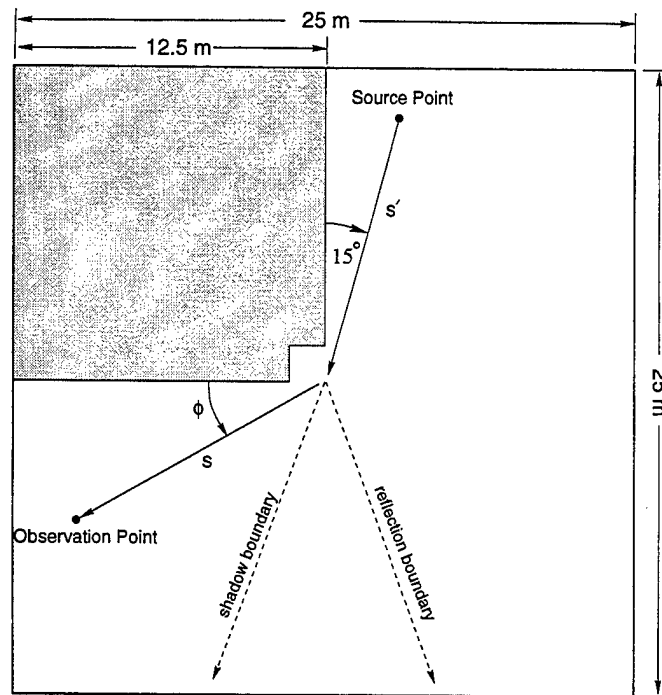


Figure 17: Notched diffracting edge

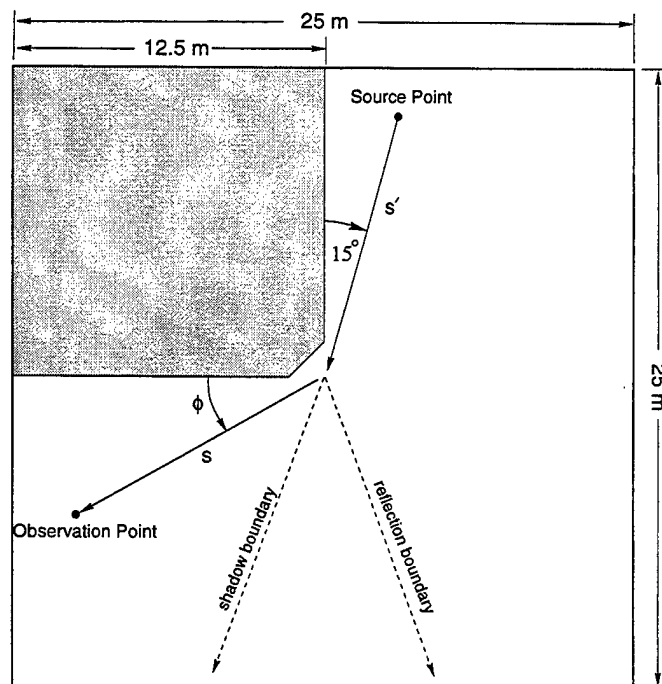


Figure 18: Beveled diffracting edge

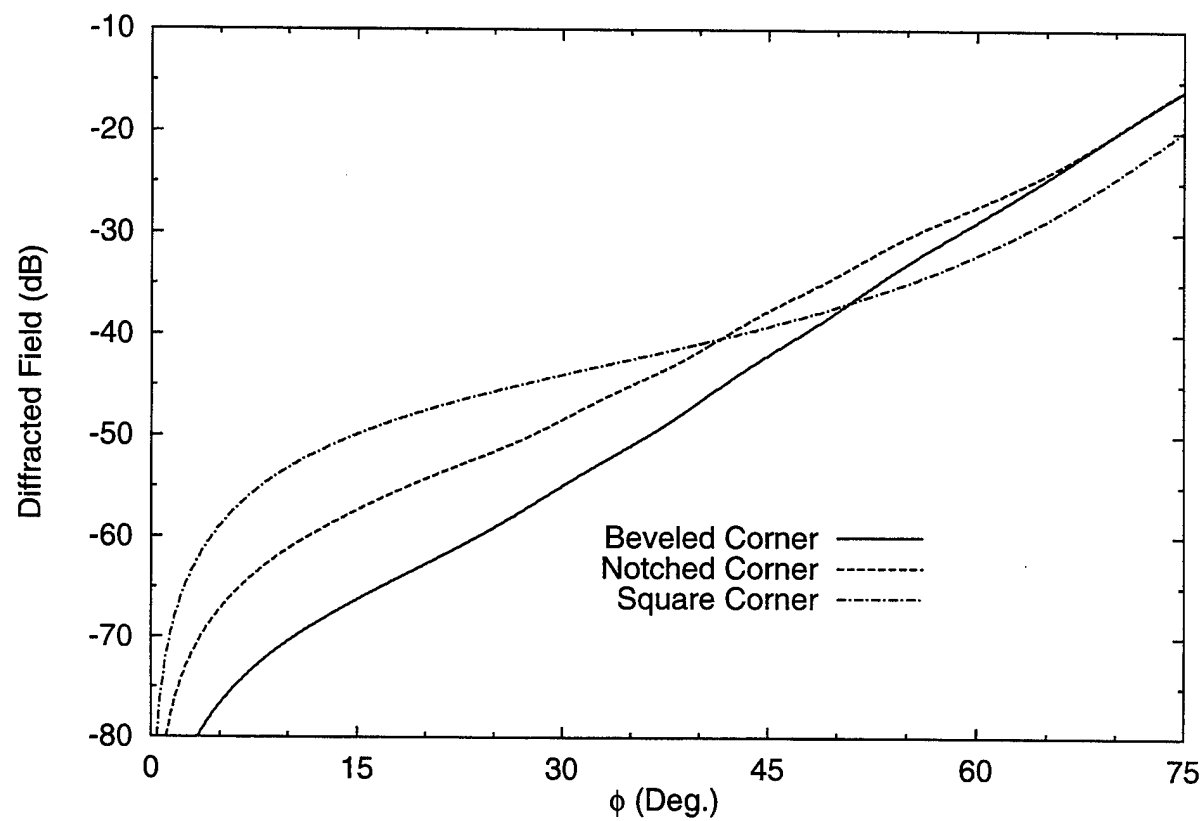


Figure 19: FDTD calculated diffracted field for different corner shapes

“notched” corner in Figure. 17, and (3) the “beveled” corner in Figure. 18. Figure 19 compares the FDTD results for the diffracted field in the shadow region ($\phi < 75$ deg.) at 900 MHz. Large differences exist among the three corner shapes, especially deep in the shadow region ($\phi < 30$ deg.). The physical explanation for this behavior is quite straightforward. For the square corner only a single diffraction takes place, but for the notched corner two diffractions must occur, and for the beveled corner the field must diffract twice as well as propagating along a lossy surface.

8. Conclusion

The results obtained in Phase I have clear potential for commercial application. During Phase I it was demonstrated that the SBR/GTD approach to propagation is both fast and accurate. Currently commercial siting methods involve extensive measurements, and even when propagation models are used, these are statistical models. They must be adapted to specific locations by using measured path loss values to set the statistical model parameters. With the SBR/GTD model, extensive measurements are not needed. This important improvement has the potential to greatly reduce the cost of siting microcellular systems while decreasing the time and effort necessary to do the site planning.

During Phase I a preliminary version of the SBR/GTD propagation model that provided results for both horizontal and vertical ray paths but with only 2D ray tracing was developed. Several improvements to the 2D and 3D ray tracing and path construction algorithms were implemented to reduce the computation time. A 2D rough terrain model was also developed for situations in which the terrain can be approximated by a two-dimensional profile, and the Tx and Rx points lie on a single vertical plane perpendicular or oblique to the ridges. A prototype computer code was also developed during Phase I for automating the construction of a linearized terrain profile starting from digitized terrain data on a rectangular grid.

During Phase I the utility of using FDTD results to validate the accuracy of the SBR/GTD model was demonstrated. Since FDTD is full wave and includes all building interactions, the FDTD results can be taken as completely accurate within the limitations of the building geometry data used for the calculations. A preliminary two-dimensional FDTD analysis made during Phase I has revealed larger than expected errors in the widely used finite conductivity Uniform Theory of Diffraction (UTD) wedge diffraction coefficients [2]. The FDTD comparisons have shown that substantial errors can occur when the diffracted ray is not near the shadow boundaries. We have also begun to use FDTD as tool for evaluating the accuracy of the ray tracing and path construction algorithms and for gaining insight into diffuse scattering from rough surfaces and on the importance of modeling small building features.

References

1. R. Luebbers, "Finite Conductivity Uniform GTD Versus Knife Edge Diffraction in Prediction of Propagation Path Loss", *IEEE Trans. Antennas Propagat.*, vol 32, no 1, pp. 70-76, January 1984.
2. R. J. Luebbers, "A Heuristic UTD Slope Diffraction Coefficient for Rough Lossy Wedges," *IEEE Trans. Antennas Propagat.*, vol. 37, no. 2, pp. 206-211, Feb. 1989.
3. R. Luebbers, "Propagation Prediction for Hilly Terrain Using GTD Wedge Diffraction", *IEEE Trans. Antennas Propagat.*, vol 32, no 9, pp. 951-955, September 1984.
4. K. A. Chamberlin and R. J. Luebbers, "An Evaluation of Longley-Rice and GTD propagation models", *IEEE Trans. Antennas Propagat.*, vol 30, no 6, pp. 1093-1098, Nov. 1982.
5. R. Luebbers, "A Semi-blind Test of the GTD Propagation Model for Reflective Rolling Terrain", *IEEE Trans. Antennas Propagat.*, vol 38, no 3, pp 403-405, March 1990.
6. R. Luebbers, J. Schuster, "Site-Specific Radio Propagation Prediction Methods for Urban Environments," Invited Paper presented at the NATO AGARD Sensor and Propagation Panel Meeting, Athens, Greece, September 18-21, 1995. Included in AGARD Conference Proceedings CP-547, "Digital Communications Systems: Propagation Effects, Technical Solutions, Systems Design," pp 41-1 to 41-14, April 1996.
7. J. Schuster and R. Luebbers, "Hybrid SBR/GTD Radio Propagation Model for Site-Specific Predictions in an Urban Environment, 12th Annual Review of Progress in Applied Computational Electromagnetics, Naval Postgraduate School, Monterey, CA, March 18-22, 1996, vol. 1, pp. 84-92.
8. K. Rizik, J. Wagen and F. Gardiol, "Two-Dimensional Ray-Tracing Modeling for Propagation Prediction in Microcellular Environments," *IEEE Trans. Veh. Technol.*, vol. 46, pp. 508-517, May 1997.
9. J. Schuster and R. Luebbers, "Comparisons of GTD and FDTD predictions for UHF radio propagation in a simple outdoor urban environment," *IEEE AP-S Intl. Symp. Proc.*, Montreal, Canada, July 13-18, 1997.